International Journal of Biological Macromolecules 127 (2019) 57–65

Contents lists available at ScienceDirect

International Journal of Biological Macromolecules

journal homepage: http://www.elsevier.com/locate/ijbiomac

Development of glycerol biosensor based on co-immobilization of enzyme nanoparticles onto graphene oxide nanoparticles decorated pencil graphite electrode

Vinay Narwal, C.S. Pundir *

Department of Biochemistry, M.D. University, Rohtak, Haryana, India

ARTICLE INFO

Article history:
Received 18 December 2018
Accepted 26 December 2018
Available online 27 December 2018

Keywords:
Glycerol
Glycerol kinase nanoparticles (GKNPs)
Glycerol 3-phosphate oxidase nanoparticles (GPONPs)
Graphene oxide nanoparticles (GrONPs)
Glycerol biosensor
Pencil graphite electrode

ABSTRACT

An improved amperometric biosensor was fabricated by immobilizing glycerol kinase (GK) and glycerol-3-phosphate oxidase (GPO) nanoparticles (NPs) onto graphene oxide nanoparticles (GrONPs) modified pencil graphite (PG) electrode. The GKNPs, GPONPs and GrONPs were characterized by UV spectroscopy, and transmission electron microscopy (TEM). The working electrode (GKNPs/GPONPs/GrONPs/PGE) was characterized by scanning electron microscopy (SEM), electrochemical impedance spectroscopy (EIS) and cyclic voltammetry (CV) techniques. The biosensor exhibited optimal current response at an applied potential of 0.45 V, pH 8.0, and 35 °C. The biosensor displayed a wide linear response for glycerol concentration from 0.001 to 60 mM with a detection limit of 0.002 μM. Moreover, a very high sensitivity 121.45 $\mu A \cdot mM^{-1} \cdot cm^{-2}$, rapid response time (2 s) and a good concurrence with the standard enzymic colorimetric technique with a correlation coefficient ($R^2 = 0.99$) was offered by the present biosensor. Evidently, biosensor revealed an analytical recovery of 98.5% after addition of glycerol to the sera samples. Within and between batches studies of working electrode demonstrated coefficients of variation of 0.098% and 0.101%, respectively. The biosensor measured blood serum glycerol level in patients suffering from hyperglyceridemia. The biosensor lost 25% of its initial activity after its regular use over a period of 210 days, at 4 °C storage condition.

1. Introduction

Glycerol, also known as Glycerin or 1,2,3-propanetriol, embraces hydroxyl (—OH) group on each of its carbon atoms. The chemical esterification of each hydroxyl group is possible in the presence of fatty acids [1]. In the liver and adipose tissue, it acts as a pioneer substrate during the synthesis of phospholipids and triglycerols. It constitutes to the storage fats of the body, which is used as source of energy by body [2]. Normal level of glycerol in human serum is 0.05–0.1 mmol/L. The elevated glycerol level over 0.327 ± 0.190 mmol/L in serum is considered as a biomarker for cardiac problems [3]. The determination of glycerol is essential in therapeutics, as its prognostic value is an important biomarker for cardiovascular diseases [4].An intensive interest in glycerol determination exists due to its extensive utility in the medical, food and biofuels industries. Various analytical methods are available for determination of glycerol, which includes gas chromatography, liquid chromatography, spectrophotometric and enzymatic methods [5–10]. The conventional methods used for glycerol detection are expensive, complex, and often lack enough specificity. Moreover, kits used in enzymatic analysis of glycerol are very costly and involve only one time use of enzymes for few sample analysis [11]. This issue has led to aquest for an accurate, rapid, and inexpensive method for quantification of glycerol. One of the sought-after methods for analyte detection is biosensing [12]. The electrochemical biosensors especially have gathered considerable attention due to their simplicity, accuracy, high selectivity, and speediness in rendering results [13,14]. In earlier reported glycerol biosensors, the native enzymes have been immobilized onto different nanocomposites, for detecting glycerol in biological fluids [15–17]. However, direct immobilization of native enzyme onto nanomaterials can cause their denaturation, and also cause harm to active binding sites of enzyme. The issue was overcome by aggregating the GK and GPO molecules into their nanoparticles and immobilizing these enzyme nanoparticles (ENPs) onto electrodes [18]. However, use of ENPs rather than native enzyme could act as a milestone in the diagnostic effectiveness of enzyme based electrodes, as ENPs showed their unique thermal and catalytic properties, beside increased surface area. These ENPs have provided promisive response in improving analytical properties of enzyme based biosensor [19]. In recent years, with the development of nanotechnology, a lot of novel nanomaterials have been fabricated and their novel properties are being gradually discovered and their

* Corresponding author.
E-mail address: chandraspundir@gmail.com (C.S. Pundir).

https://doi.org/10.1016/j.ijbiomac.2018.12.253
0141-8130/

applications have also greatly advanced biosensors [20]. Due to the exceptional electronic, optical, mechanical, and thermal properties, graphene nanomaterials have shown great promises in a wide range of applications. Graphene derivatives, e.g. graphene oxide and reduced graphene oxide sheets, possess surface defects and oxygen functional groups, which renders it ideal templates for synthesis of metal and semiconductor nanoparticles. Graphene-nanoparticle composites are expected to show enhanced properties, which arise from the synergic effect of the graphene oxide/reduced graphene oxide sheets and the anchored nanoparticles [21]. By combining these unique and robust materials with enzyme nanoparticles, a striking synergy can often be achieved. Pencil graphite (PG) electrode possesses various fascinating characteristics for instance high conductivity, cost effectiveness, low signal to noise ratio and easy accessibility, which renders it a better option over electrodes such as Au, glassy-carbon and Pt electrodes [22]. Hence, we describe herein the fabrication of an ultrasensitive, rapid and cost effective glycerol biosensor based on co-immobilization of nanoparticles (NPs) of glycerol kinase (GK) and glycerol-3-phosphate oxidase (GPO) onto GrONPs decorated PGE for detection of glycerol in hyperglyceridemia patients.

2. Materials and methods

2.1. Experimental methods

2.1.1. Materials

Glycerol, ascorbic acid, uric acid, glycine, acrylamide, glucose, silica gel from SRL, Mumbai, H_2SO_4, $KMNO_4$, $NaNO_3$, H_2O_2 and HCl from Qualigens Fine Chemicals, Mumbai were used. 6B graphite pencil (Make: Camlin, India) with a graphite rod of 2 mm diameter was bought from the local stationary market. Distilled water (DW) (ohmic resistance: 1.8×10^{-5} for every ohm) was used throughout the study. The sera samples from apparently healthy people and cardiac patients were taken from local Pandit Bhagwat Dyal Sharma Post Graduate Institute of Medical Science (Pt.BDS PGIMS) hospital.

2.1.2. Instruments used

Potentiostat/Galvanostat (Make: Autolab, model: AUT83785, made by Eco Chemie, The Netherland) with NOVA 1.4 software was used. UV Spectrophotometer (Make: Shimadzu, Japan, Model 1700), Scanning electron microscopy (SEM) (Zeiss EV040, USA), were utilized. The electrochemical impedance spectra (EIS) was recorded by FRA software in 5 mM $K_3Fe(CN)_6/K_4Fe(CN)_6$, 25 ml solution at −0.2 V between frequency range, 0.01 Hz–10 kHz.

2.1.3. Preparation of GrONPs

GrONPs were prepared by Hummer's method, with slight modifications. Graphene rod from a HB pencil was crushed to a powder in a pestle mortar. Graphite powder (5.0 g), $NaNO_3$ (3.75 g) and $KMNO_4$ (15.0 g) were mixed in a 2 L conical flask. Concentrated H_2SO_4 (375 mL) was added slowly to the flask and kept under constant stirring for 5 days at room temperature, 5% H_2SO_4 (1.0 L) was added and kept at 98 °C in a heating mantle for 2 h. The mixture was cooled to 60 °C and 30% H_2O_2 (30 mL) was added, stirred it for another 2 h and centrifuged at 10,000 rpm for 15 min to collect the bottom product i.e. GrONPs. The GrONPs were washed with 0.5% H_2O_2 (10 times) followed by 5% HCl solution (5 times) and then with DW until the pH of supernatant was neutral. Finally the GrONPs were dried in vacuum oven to obtain their light brown powder [21].

2.1.4. Preparation of GKNPs and GPONPs

The GKNPs and GPONPs were synthesized separately using desolvation method [23]. To 3 mL solution of GK and GPO, absolute ethanol was added slowly in dropwise manner i.e. 0.1–0.2 mL/min with constant stirring rate i.e. 500 rpm. The process was followed by the addition of 1 mL, 2.5% glutaraldehyde solution in the mixture under the identical stirring conditions at 4 °C for 24 h to ensure complete crosslinking of respective ENPs. The glutaraldehyde provided intermolecular crosslinking of enzyme molecules via Schiff base. The synthesized ENPs were thiol functionalized by adding 0.2 mL of cysteamine solution (0.02 g/mL) to each suspension under constant stirring for 5–6 h. ENPs were precipitated from mixture by centrifugation NPs mixture at 1200 ×*g* for 10 min at 4 °C. The process was followed by dispersion of ENPs in 2 mL 0.1 M phosphate buffer, pH 7.3 and sonication for 5 min. It was assumed that alpha-NH_2 group of cysteamine reacts with excess unreacted —CHO groups of glutaraldehyde cross-linked ENPs to form Schiff base. Thus, the glutaraldehyde cross-linked ENPs get functioned with —NH_2 groups. These functionalized ENPs were stored at 4 °C, until use.

2.1.5. Characterization of GrONPs, GKNPs and GPONPs

GrONPs, GKNPs and GPONPs characterization were done by recording their images using transmission electron microscope (TEM), and UV–visible spectra (200–600 nm).

2.1.6. Preparation of GrONPs/GKNPs/GPONPs/PG electrode

The GrONPs, GKNPs and GPONPs modified PG electrode was prepared by covalent immobilization of enzyme nanoparticles onto the surface of pencil graphite electrode. The bare PG electrode was pretreated with a potential range of −1.1 to 0.1 V in solution of freshly prepared 0.2 M H_2SO_4, until the cyclic voltammogram characteristics of the bare PG electrode was developed. The surface of PG electrode (diameter 2 mm) was polished manually by alumina slurry (diameter 0.05 μm) with a polishing cloth, followed by thorough washing with distilled water (DW). This electrode was then treated with piranha solution (3 mL H_2SO_4:1 mL H_2O_2) followed by placing it into ethanol and sonicated to remove adsorbed particles. The prepared GrONPs (1 mg) were dispersed into 25 ml of 0.1 M KOH solution and then stirred continuously for 2 h at 92 °C. The dispersed GrONPs were electrodeposited onto surface of PGE through cyclic voltammetry in a Potentiostat/Galvanostat by applying 20 successive polymerization cycles at −1.1 to 0.1 V at a scan rate of 20 mV/s The resulting GrONPs modified PGE was washed thoroughly with DW to remove unbound matter. The GrONPs modified PG electrode was dipped into the GKNPs and GPONPs suspension at 4 °C for 24 h to get co-immobilization of ENPs onto PG electrode. The GrONPs/GKNPs/GPONPs/PG electrode was washed with 0.1 M of sodium phosphate buffer (SPB, pH 7.0) to remove extra molecules of ENPs. The working electrode was stored in the SPB (pH 7.0) buffer at 4 °C, when not in use. The GrONPs/GKNPs/GPONPs/PG electrode was characterized using techniques SEM and EIS before and after its immobilization with ENPs.

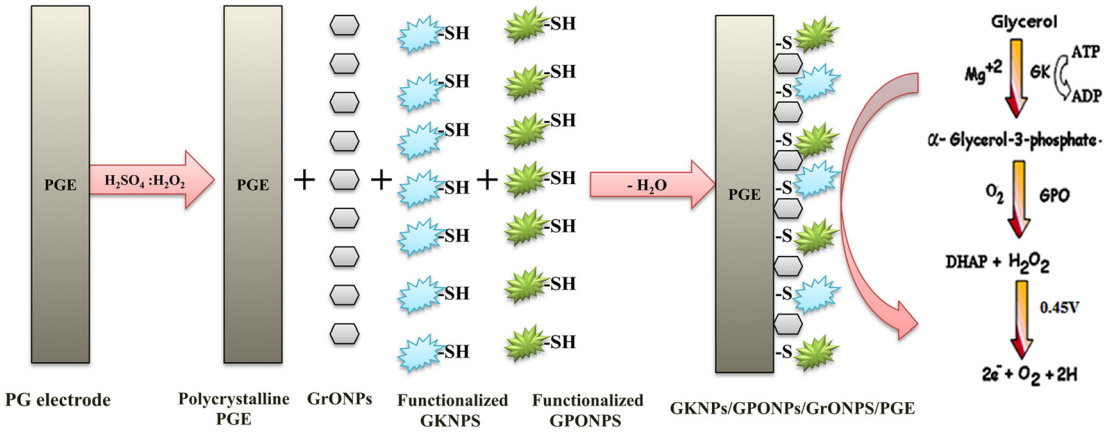

Fig. 1. Schematic representation of step by step construction procedure of an amperometric glycerol biosensor based on GrONPs/GKNPs/GPONPs/PGE.

2.1.7. Fabrication of glycerol biosensor and its response measurements

An amperometric glycerol biosensor was fabricated using GKNPs/GPONPs/PG electrode as working electrode, Ag/AgCl as standard electrode and Pt wire as an auxiliary electrode connected through galvanostat/potentiostat. Fig. 1 represents the schematic presentation of construction of working electrode and electro-chemical reactions involved in its response measurement. The working electrode was optimized and characterized using various cyclic voltammetry methods. All electrochemical procedures were performed in 0.1 M phosphate buffer containing 0.1 mM (0.1 mL) glycerol and optimized concentration of ATP and $MgCl_2$ at an optimized scan rate. The current response was measured between 0 s and 10s.

2.1.8. Optimization of glycerol biosensor

The kinetic properties such as ATP concentration, $MgCl_2$ concentration, applied potential, scan rate, pH, temperature and effect of glycerol concentration of GrONPs/GKNPs/GPONPs/PG electrode were studied electrochemically to optimize the operational conditions of the biosensor. The concentrations of ATP and $MgCl_2$ were varied from 0.1 to 4.0 mM to get the meaningful response at optimum concentrations. Similarly, effect of scan rate was studied between 5 mV/s to 20 mV/s. To get the optimum pH, the pH was varied in the range pH 6.0 to 9.0 at an interval of pH 0.5 using the suitable buffers (strength-0.1 M). Likewise to get optimum temperature and incubation time the master mix (buffers, substrate, ATP and $MgCl_2$) was incubated at different temperature (20–50 °C) and time duration (0–10s). The effect of glycerol concentration on biosensor response was determined by varying the concentration of glycerol in the range, 0.1 mM–70 mM. The limit of detection (LOD) was calculated using the equation: LOD = 3xσ/slope, where σ = standard deviation.

2.1.9. Evaluation of glycerol biosensor

The evaluation of the working electrode was done by analyzing its analytical performance in terms of analytical recovery, reproducibility, precision and correlation coefficient. The analytical recovery and coefficient of variation were calculated by the equations:

$$\%\text{Recovery} = \frac{\text{Conc. of serum glycerol estimated after addition of exogenous glycerol}}{\text{Conc. of glycerol in serum before addition} + \text{conc. of added exogenous glycerol}} \times 100$$

$$\text{Coefficient of variation} = \frac{\text{Standard deviation} \times 100}{\text{Mean of samples}}$$

The effect of various interferants found in the blood such as glucose, glutamic acid, ascorbic acid and urea were measured at their physiological concentrations into the blood.

2.1.10. Application of glycerol biosensor

Blood samples (1 mL each) of apparently healthy people's and patients suffering from hyperglyceridemia in different age groups (n = 20 each) were collected from local Pt. BDS PGIMS, Rohtak Hospital. The hospital has ethical clearance from competent ethical committee/board to collect samples from outdoor patients. The samples were centrifuged at 5000 ×*g* for 5 min to get their supernatants (sera) and kept at 4 °C until use. The quantity of glycerol in sera was measured by the present biosensor in the same fashion as elucidated above for its response measurement, under optimized operational conditions except that serum was used instead of glycerol. The current (mA) was recorded and the quantity of glycerol in serum was interposed from the standard curve between glycerol concentrations and current (in mA) under optimal operational conditions (Fig. 2a).

2.1.11. Storage stability of enzyme electrode

The storage stability and long term stability of the biosensor were analyzed during its regular use over a period of 210 days, while its storage at 4 °C.

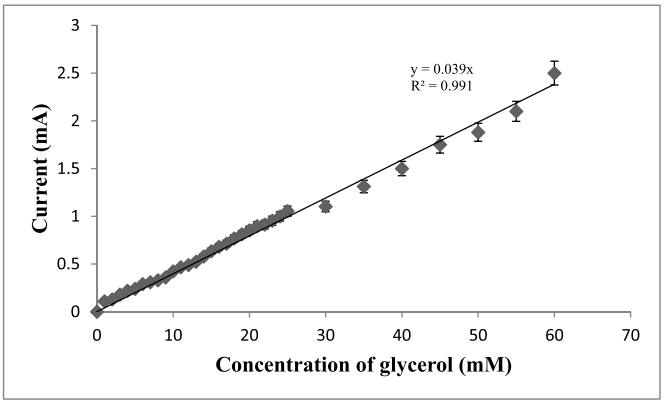

a

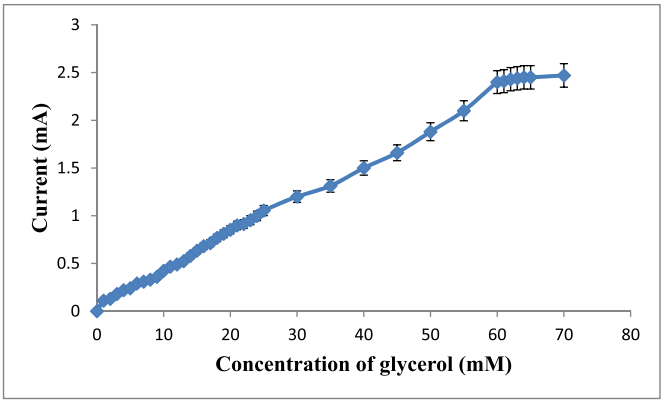

b

Fig. 2. (a) Calibration curve of glycerol measured by the GrONPs/GKNPs/GPONPs/PGE. Measuring conditions: 0.1 M sodium phosphate buffer (SPB), pH 8.0, potential 0.45 V vs Ag/AgCl electrode. (b) Effect of glycerol concentrations on current response of GrONPs/GKNPs/GPONPs/PG electrode. All readings are mean of five observations (n = 5).

3. Results

3.1. Characterization of GrONPs, GKNPs and GPONPs

The size of GrONPs, GKNPs and GPONPs as measured by TEM was in the range, 5 to 100 nm (Fig. 3a), with an average size of 20 nm. UV and visible spectra of GrONPs exhibited absorbance peak at 230 nm, while GKNPs and GPONPs showed strong absorbance peak at 280 nm respectively (Fig. 3b).

3.2. Characterization of GrONPs/GKNPs/GPONPs/PG electrode

3.2.1. By scanning electron microscopy (SEM)

Fig. 3c showed the SEM images of bare PG electrode, and GrONPs/GKNPs/GPONPs modified PG electrode at a magnitude of 100 nm. Bare electrode depicted the smooth and flat morphology, whereas GrONPs/GKNPs/GPONPs/PG electrode revealed globular structural morphology. The globular morphology was due to enzyme nanoparticles of GK and GPO, which were clearly adsorbed in transparent pencil graphite electrode.

3.2.2. By electrochemical impedance spectroscopy (EIS)

The EIS provides the change in impedance of electrode before and after its modification with immobilization of GKNPs/GPONPs. The semicircle diameter at higher frequencies contributed to the electron transfer resistance (R_{CT}), which directed the electron transfer kinetics of the redox probe at the surface of electrode, while at lower frequencies linear part corresponded to Warburg diffusion process. In Fig.3d, the Nyquist plot presented EIS of bare PG electrode, GrONPs/PG electrode and GrONPs/GKNPs/GPONPs/PG electrode in 5 mM ($K_3Fe(CN)_6/K_4Fe(CN)_6$) respectively. The R_{CT} value for the bare PG electrode is 120 Ω, which got reduced after electrodeposition of GrONPs up to 40 Ω due to high electrical conductivity of GrONPs while it further gets increased after co-immobilization of GKNPs/GPONPs onto GrONPs/PG electrode up to 225 Ω which was due to high insulation capability of GKNPs and GPONPs.

3.3. Voltammetric response of the GrONPs/GKNPs/GPONPs/PG electrode

The unmodified/bare PG electrode had showed very low current, while on the contrary, a well defined oxidation and reduction current appeared for GrONPs/GKNPs/GPONPs/PG electrode at a potential of 0.45 V(Fig. 4a). The current increases linearly with increase in scan rate from 20 mV/s to 40 mV/s (Fig. 4b). At scan rate of 20 mV/s both oxidation and reduction current appeared as compared to higher scan rate. Hence, all electrochemical studies were performed at an optimized scan rate of 20 mV/s.

3.4. Current response measurement of GrONPs/GKNPs/GPONPs/PG electrode

The amperometric response of the GrONPs/GKNPs/GPONPs/PG electrode was analyzed as a function of glycerol concentration (0.1 mM) by measuring CV at 20 mV/s scan rate in 0.1 M PBS of pH 7.0 containing 5 mM [Fe(CN)6]3−/4− (the electrical conductivity of PBS = 25 Ω). Glycerol biosensor was based on the principle of measurement of electrons which were produced from H_2O_2 at a fixed potential. The GKNPs in the presence of ATP and $MgCl_2$ phosphorylated glycerol into glycerol-3-phosphate. Further, GPONPs oxidized glycerol-3-phosphate into dihydroxyacetone phosphate and H_2O_2. The electron i.e. current is generated from electro-oxidation of H_2O_2 under low potential, which is measured. The amperometric response of PG electrodes without and with a mixture of ENPs (with substrate and without substrate) was recorded. At a glycerol concentration of 10 mM, the amperometric response of the PG electrode with native enzymes (GK/GPO) was 0.17 mA, while the same electrode with mixture of ENPs (GKNPs/GPONPs) was 1.86 mA.

3.5. Optimization of glycerol biosensor

An amperometric biosensor was constructed by decorating GKNPs and/GPONPs onto PG electrode. The optimum concentration of ATP was determined by investigating the response of biosensor at different ATP concentrations, when applied for 0.1 mM glycerol. The maximum current was predicted at 1.5 mM concentration of ATP (Fig. 4c). Thus, 1.5 mM ATP concentration was kept for further work. Similarly, optimized $MgCl_2$ concentration was found 3.0 mM $MgCl_2$ for ensuing work (Fig. 4d), which was comparable with GK/GPOx/Horse Radish Peroxidase (3.00 mM) biosensor [15]. The maximum current was observed within 2 s at 0.45 V against Ag/AgCl (Fig. 5c). The biosensor expressed the optimum current at pH 8.0, incubation temperature 35 °C in 0.1 M sodium phosphate buffer (Fig. 5a and 5b). While at other lower and higher pH and temperature there was gradual shift in the oxidation and reduction peaks with decline in the current range. Hence, the succeeding electrochemical studies for glycerol detection were performed in 0.1 M sodium phosphate buffer of pH 8.0 and temperature 35 °C at optimal potential of 0.45 V. The response of current for GrONPs/GKNPs/GPONPs/PG electrode increases linearly with increase in glycerol concentration. At high concentration of glycerol, a plateau current is perceived, depicting the feature of Michaelis–Menten kinetic process. The apparent Michaelis–Menten constant (Km), provided the evidence of enzyme substrate kinetics, which can be attained through the Lineweaver–Burk equation

$$\frac{I}{I_{ss}} = \frac{I}{I_{max}} + \frac{Km}{I_{max}C}$$

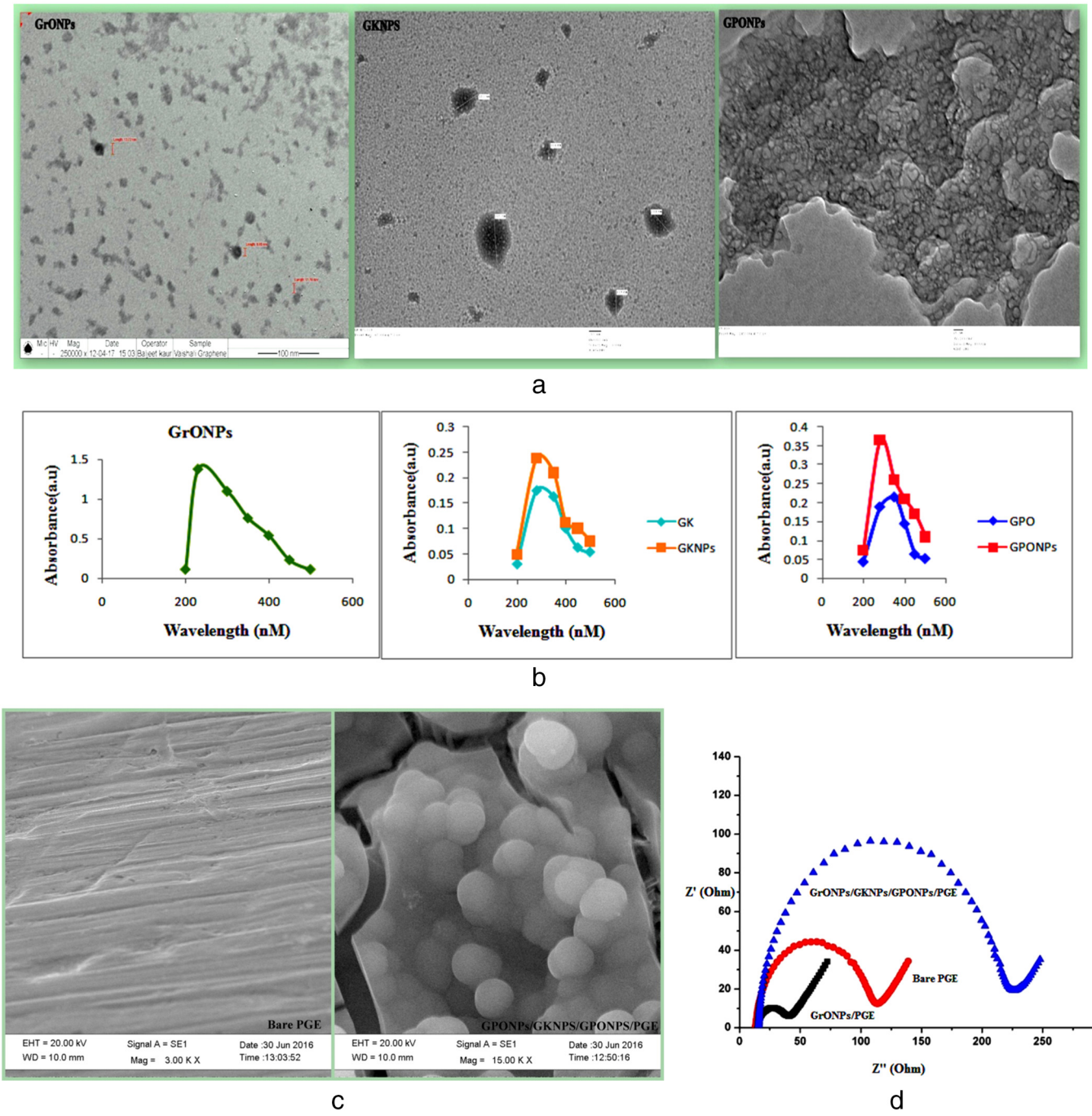

Fig. 3. (a) Transmission electron microscopic (TEM) images of GrONPs, GKNPs, and GPONPs. (b) UV absorbance of GrONPs, GKNPs and GPONPs. (c) Scanning electron microscopic (SEM) images of bare PG electrode, and GrONPs/GKNPs/GPONPs/PG electrode (Pure ethanol was used as fixative and samples were prepared by pasting electrode onto carbon tape modified grid). (d) Electrochemical Impedance Spectra (EIS) of a) bare electrode b) GrONPs /PG electrode c) GrONPs/GKNPs/GPONPs/PG electrode.

Here, I_{ss} indicated steady-state current after addition of substrate, C represented the bulk concentration of the substrate, and I_{max} showed the maximum current sustained under saturated substrate conditions. The GrONPs/GKNPs/GPONPs/PG electrode exhibited a I_{max} of 6.86 ± 0.12 mA with app. Km of 0.1 ± 0.1 mM and showed high sensitivity of 121.45 $\mu A \cdot mM^{-1} \cdot cm^{-2}$ at a potential of 0.45 V.

3.6. Evaluation of glycerol biosensor

The biosensor offered a linear response between current (mA) and wider glycerol concentration range of 0.01 mM–60 mM, under optimized operational conditions (Fig. 2b). The limit of detection limit (LOD) of the present biosensor was 0.002 μM. The analytical recoveries of added glycerol in sera at concentration of 0.5 mM and 1.0 mM were 96.3 and 98.55% respectively (Table 1). In addition, within and between batch coefficients of variation for working electrode were detected as 0.098% and 0.101%, respectively (Table 2).

3.7. Correlation of glycerol biosensor

The glycerol level detected by the present biosensor was also compared with the standard enzymic colorimetric kit method. A good

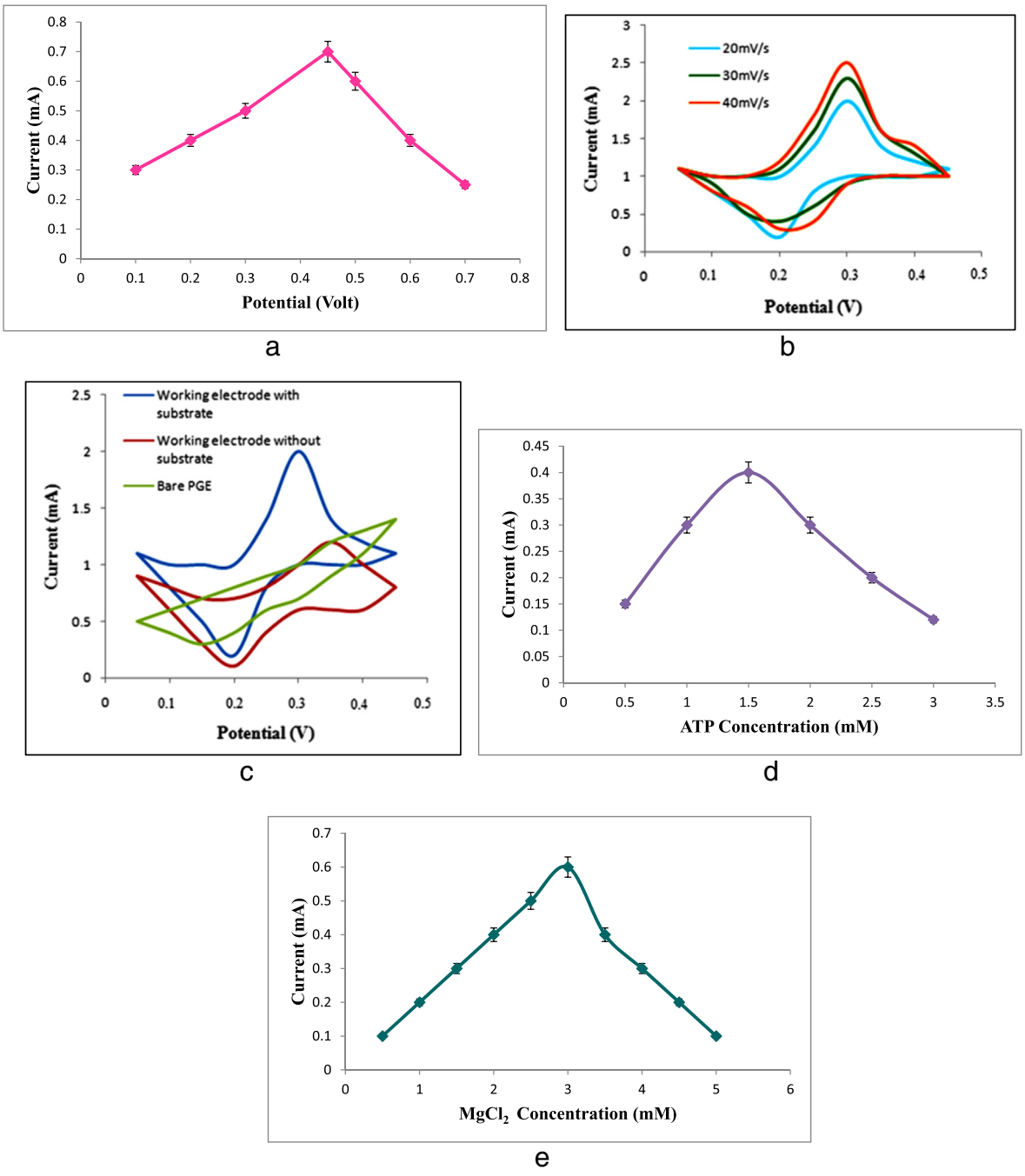

Fig. 4. (a) Effect of applied potential on GrONPs/GKNPs/GPONPs/PG electrode containing, 1 mM ATP, 2 mM $MgCl_2$ and 0.1 mM glycerol. (b) Effect of scan rate on GrONPs/GKNPs/GPONPs/PG electrode containing, 1 mM ATP, 2 mM $MgCl_2$ and 0.1 mM glycerol. (c) Cyclic voltammetry of bare PGE, GrONPs/GKNPs/GPONPs/PG electrode with or without substrate. (d) Effect of the ATP concentration in the buffer solution (containing 2 mM $MgCl_2$) on the amperometric signal of 0.1 mM glycerol at GrONPs/GKNPs/GPONPs/PG electrode. (e) Effect of $MgCl_2$ concentration in the buffer solution (containing 1 mM ATP) on the amperometric signal of 0.1 mM glycerol at GrONPs/GKNPs/GPONPs/PG electrode.

correlation coefficient ($R^2 = 0.99$) was obtained between the present method and standard enzymic colorimetric kit method (Fig. 6a).

3.8. Application of glycerol biosensor

The quantity of sera glycerol in apparently healthy persons as detected by the current biosensor was in the range 0.03 ± 0.01–0.3 ± 0.02 ($n = 20$) mM, which was in normal established range. The sera glycerol level in persons suffering from cardiogenic shocks was in the range 1.5 ± 0.01–15 ± 0.01 mM ($n = 20$), which was notably higher than the levels in apparently healthy persons ($p > 0.001$) (Table 3).

3.9. Interference study of glycerol biosensor

Interfering components like glucose, glutamic acid, uric acid, ascorbic acid and urea had basically no effect on glycerol biosensor response at their physiological concentrations, under the standard assay conditions. The interference obtained was <5%, which had no significant effect on the amperometric response of the present biosensor.

3.10. Storage stability of the GKNPs/GPONPs/PG electrode

The storage stability of working electrode was investigated by measuring the response of glycerol concentration (0.01 mM) in 0.1 M PBS

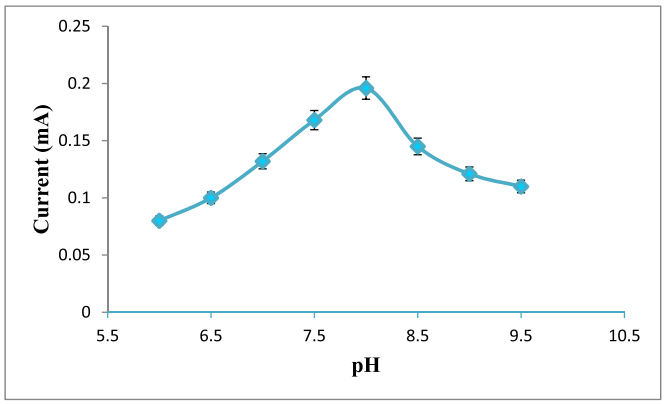

a

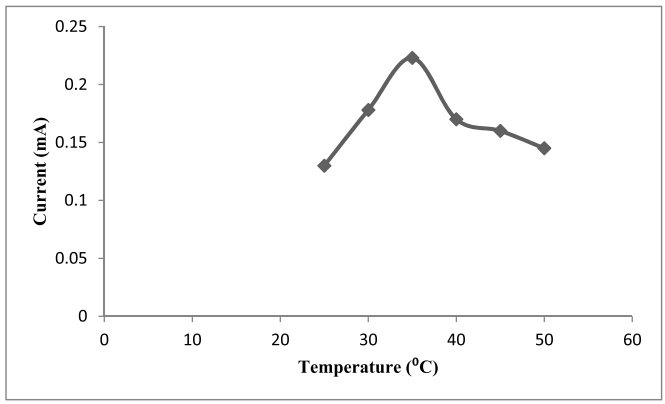

b

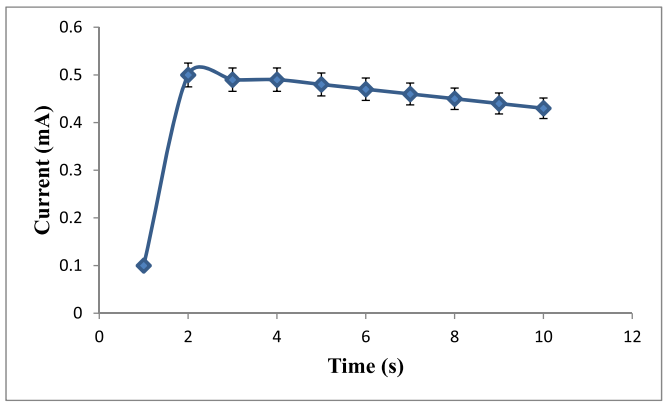

c

Fig. 5. (a) Effect of pH on GrONPs/GKNPs/GPONPs/PG electrode containing, 1 mM ATP, 2 mM $MgCl_2$ and 0.1 mM glycerol. (b) Effect of temperature on GrONPs/GKNPs/GPONPs/PG electrode containing, 1 mM ATP, 2 mM $MgCl_2$ and 0.1 mM glycerol. (c) Effect of incubation time on GrONPs/GKNPs/GPONPs/PG electrode containing, 1 mM ATP, 2 mM $MgCl_2$ and 0.1 mM glycerol.

for 7 weeks (Fig. 6b). The biosensor showed no change in redox peaks, current and potential during 4 weeks, but showed a drop in the value of the current in last 2 weeks it without any change in redox peaks

Table 1
Analytical recovery of added glycerol in the serum samples (n = 5), as measured by glycerol biosensor based on GrONPs/GKNPs/GPONPs/PG electrode.

Glycerol added (mM)	Glycerol found (mM)	% Recovery
–	1.78	–
0.5	2.2	96.3 ± 0.1
1.0	2.76	98.55 ± 0.1

Table 2
Within and between assay coefficients of variation (CV) for determination of glycerol in the serum samples (n = 5), as measured by glycerol biosensor based on GrONPs/GKNPs/GPONPs/PG electrode.

N	Glycerol (mM)	CV (%)
Within assay (5)	26.1 ± 0.1	0.098
29		
28		
27		
24		
23		
Between assay (5)	20.2 ± 0.2	0.101
19		
18		
20		
23		
22		

and potential. On that account, biosensor lost 25% of its initial activity during 7 months of its 250 reuses, while being stored at 4 °C. The biosensor fabrication reproducibility was checked for three electrodes by determining response of 0.01 mM glycerol by cyclic voltammetry. The relative standard deviation (RSD) for the current response was 1.53%.

4. Discussion

In the present work, we prepared NPs of GrONPs, glycerol kinase (GK) and glycerol-3-phosphate oxidase (GPO), characterized and co-immobilized them onto PG electrode to fabricate an improved

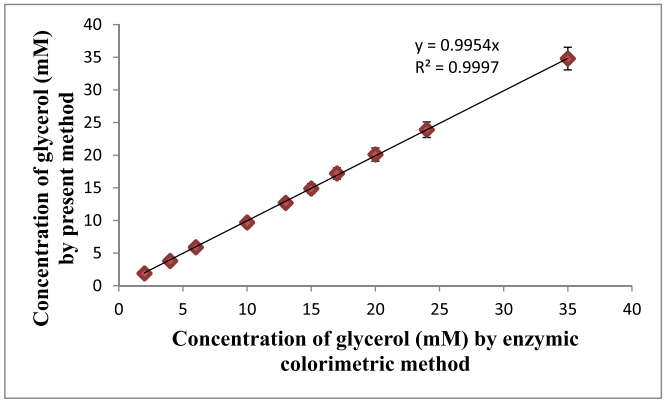

a

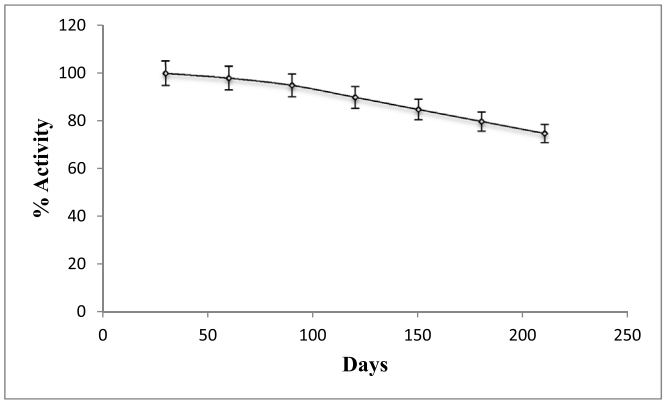

b

Fig. 6. (a) Correlation between serum glycerol level measured by enzo kit method (x axis) and the current method (y axis) employing the glycerol biosensor based on GrONPs/GKNPs/GPONPs/PG electrode. (b) Storage stability of GrONPs/GKNPs/GPONPs/PG electrode at 4 °C.

Table 3
Serum glycerol levels in apparently healthy persons and cardiogenic shocks patients, as measured by glycerol biosensor based on GrONPs/GKNPs/GPONPs/PG electrode.

Sex	Age (year)	Apparently healthy persons (mM)	Sex	Age (year)	Hypertriglyceridemia patients (mM)
M	54	0.04 ± 0.02	M	39	1.5 ± 0.01
F	34	0.06 ± 0.01	M	55	5.9 ± 0.03
M	56	0.3 ± 0.02	F	56	9.4 ± 0.02
M	60	0.05 ± 0.02	M	49	12.2 ± 0.03
M	64	0.09 ± 0.01	F	63	7.6 ± 0.02
M	43	0.06 ± 0.02	M	48	6.3 ± 0.03
F	32	0.04 ± 0.01	M	29	8.6 ± 0.01
M	39	0.09 ± 0.02	F	45	7.1 ± 0.04
M	52	0.09 ± 0.01	M	43	8.6 ± 0.02
F	54	0.08 ± 0.02	M	46	6.3 ± 0.01
M	45	0.06 ± 0.02	F	36	7.3 ± 0.05
M	44	0.04 ± 0.01	M	42	12.1 ± 0.01
M	47	0.03 ± 0.01	F	34	13 ± 0.02
F	39	0.07 ± 0.01	M	59	12 ± 0.02
M	41	0.2 ± 0.01	M	67	14 ± 0.01
F	39	0.1 ± 0.01	M	59	15 ± 0.01
F	37	0.2 ± 0.02	M	49	6.0 ± 0.02
M	58	0.04 ± 0.05	F	44	12.6 ± 0.01
M	68	0.06 ± 0.02	M	39	11.2 ± 0.02
F	55	0.07 ± 0.02	F	58	12.4 ± 0.01

amperometric biosensor for determination of glycerol. The average size of GrONPs, GKNPs and GPONPs (20 nm, range 5–100 nm) (Fig. 3a) revealed the enhanced surface area of enzymes as compared to the native GK and GPO molecules. A strong absorbance peak of GrONPs at 230 nm and GKNPs &GPONPs at 280 nm (Fig. 3b), showed a high degree of absorption of aromatic amino acids of peptide chain/free enzyme following their NPs formation. The change of smooth and featureless morphology of PG electrode to globular structure after immobilization of GKNPs and GPONPs as seen in SEM images (Fig. 3c) was due to adsorption of GKNPs/GPONPs onto GrONPs modified PG electrode. The porous electrode revealed larger and effective surface area after absorption of GKNPs/GPONPs. The increased R_{CT} value of GrONPs/GKNPs/GPONPs/PG electrode was due to high surface area and good electrical properties of enzyme nanoparticles. This increase in R_{CT} could be assigned to the reason that most biological molecules, including enzyme nanoparticles, have poor electrical conductivity at low frequencies (<10 kHz; applied voltage: 0.45 V) and create obstacle to the transfer of electrons. However, GrONPs/GKNPs/GPONPs offer high surface to volume ratio and increase in the electrocatalytic property of electrode for electro-oxidation of glycerol. At 10 mM glycerol concentration, the current response of the GrONPs/GKNPs/GPONPs/PG electrode was 1.86 mA, which is higher than that with native enzymes (GK/GPO) (0.17 mA), which revealed that the hybrid ENPs had an enormous effect towards the analytical response of working electrode. The highest current of present biosensor was observed at 1.5 mM ATP, which is comparable with previously reported biosensor GK/GPOx/Horse Radish Peroxidase (1.5 mM) [15]. Similarly for $MgCl_2$, the biosensor required 3.0 mM concentration for optimum response (Fig. 4d), which is comparable with GK/GPOx/Horse Radish Peroxidase (3.00 mM) biosensor [15]. The maximum current was observed within 2 s at 0.45 V against Ag/AgCl. The app. Km of GKNPs/GPONPs/PG electrode for glycerol was 0.1 ± 0.01 mM. The small Km value means that the immobilized ENPs at PG electrode possess a high affinity to glycerol. The wide working range of the biosensor 0.001 mM–60 mM, under optimum conditions (Fig. 2b), is better than earlier biosensors (1 μM–20 μM, 1 to 25 mM and 0.05 to 25.6 mM [15–17].The LOD of the present biosensor (0.002 μM), was also better than earlier biosensors (0.4 μM, 0.005 mM and 0.05 mM [15–17]. The high recoveries of added glycerol in sera (96.3–98.55%) (Table 1) demonstrated the reliability of the present biosensor. Very low values of within and between batch coefficient of variation for the added glycerol in sera measured by the present biosensor was 0.098% and 0.101%, respectively (Table 2). The excellent reproducibility exhibited by the biosensor is due to electrostatic interaction of GrONPs/GKNPs/GPONPs onto PG electrode. Furthermore, the working electrode displayed a correlation coefficient of $R^2 = 0.99$ between sera glycerol quantity detected with the standard enzymic colorimetric method and present biosensor method, revealed the high accuracy of the present biosensor. The biosensor had good anti-interferent ability which was owing to better operational conditions for instance low potential (0.45 V) and higher current. The interfering components lost their activity at such a low potential and current, which evidenced the high specificity of present biosensor. A < 25% decrease in the activity of GrONPs/GKNPs/GPONPs/PG electrode at its everyday use during a period of 7 weeks, while being stored dry at 4 °C, which showed higher storage stability of the enzyme electrode over earlier reported electrodes. It was due to the uniform immobilization of ENPs onto the PGE. Furthermore, graphite present in PGE could offer a biocompatible environment, which inhibits the denaturation of enzyme nanoparticles.

5. Conclusion

In the present study, the better electroanalytical properties and improved analytical performance was achieved using enzyme nanoparticles (ENPs) in place of native enzymes and GrONPs. The ENPs exhibited high surface to volume ratio, which allow a large electroactive surface of PGE. The large electroactive surface area of GrONPs/GKNPs/GPONPs/PGE has contributed in improved analytical performance of biosensor in terms of rapid response rate (2 s), low detection limit (0.002 μM), wide linear response (0.001 mM to 60 mM) and prolonged storage stability (210 days). The improved analytical performance of biosensor can be accredited to the large surface area, good biocompatibility and high electrical conductivity of PGE. The PGE allows the uniform immobilization of ENPs, retain their bioactivity and increases the direct electron flow from H_2O_2. Thus, enzyme nanoparticles modified PGE could also be used to improve analytical performance of other biosensors also.

Acknowledgement

The authors are grateful to Council of Scientific and Industrial Research (CSIR), New Delhi-110012 for providing financial support to this work.

Conflict of interest

Authors have no conflict of interest.

References

[1] M. Pagliaro, Glycerol, Glycerol (2017) 109–132, https://doi.org/10.1016/b978-0-12-812205-1.00005-9.
[2] K. Koehler, H. Braun, M.D. Marees, H. Geyer, M. Thevis, J. Mester, et al., Glycerol administration before endurance exercise: metabolism, urinary glycerol excretion and effects on doping-relevant blood parameters, Drug Test. Anal. 6 (2013) 202–209, https://doi.org/10.1002/dta.1446.
[3] A. Christophe, F. Matthus, Determination of serum glyceride glycerol, Bull. Soc. Chim. Belg. 73 (2010) 592–596, https://doi.org/10.1002/bscb.19640730526.
[4] G. Iacobellis, Epicardial fat thickness as a biomarker in cardiovascular disease, Biomark. Cardiovasc. Dis. (2016) 1097–1107, https://doi.org/10.1007/978-94-007-7678-4_13.
[5] K. Kurahashi, K. Hisada, M. Kashiwagi, S. Yoshihara, T. Nomura, H. Tokumoto, Analysis of the continuous bioconversion of glycerol by promotion of highly glycerol-resistant glycerol-degrading Bacteria, Waste Biomass Valori. (2018)https://doi.org/10.1007/s12649-018-0344-4.
[6] N. Kiba, H. Maruyama, M. Furusawa, Improved high-performance liquid chromatographic method with fluorimetric detection for the determination of glycerol using an immobilized enzyme column reactor, J. Chromatogr. A 456 (1988) 398–404, https://doi.org/10.1016/0021-9673(86)80038-3.
[7] C.S. Frings, H.L. Pardue, An automatic spectrophotometric method for the enzymatic determination of glycerol, Anal. Chim. Acta 34 (1966) 225–228, https://doi.org/10.1016/s0003-2670(00)89030-3.
[8] C. Cordella, Computer-aided determination of glycerol in food products with GlycerolSoft, a tool for assessing the quality of food, TrAC Trends Anal. Chem. 22 (2003) 115–122, https://doi.org/10.1016/s0165-9936(03)00209-7.

[9] B. Merchie, A. Girard, B. Maisterrena, P. Michalon, R. Couturier, Reliable amperometric determination of glycerol and glycerol-3-phosphate with a bienzymatic nylon membrane electrode, Anal. Chim. Acta 263 (1992) 85–91, https://doi.org/10.1016/0003-2670(92)85429-a.
[10] L.J. Murphy, P.T. Galley, Measurement in vitro of human plasma glycerol with a hydrogen peroxide detecting microdialysis enzyme electrode, Anal. Chem. 66 (1994) 4345–4353, https://doi.org/10.1021/ac00095a035.
[11] M. Gündogan-Paul, H. Özyörük, S. Çelebi, A. Yildiz, Amperometric Enzyme Electrode for Hydrogen Peroxide Determination Prepared with Horseradish Peroxidase Immobilized in Polyvinylferrocenium (PVF), Electroanalysis 14 (2002) 505–511, https://doi.org/10.1002/1521-4109(200204)14:7/8<505::aid-elan505>3.0.co;2-#.
[12] A. Manzoni, Application of immobilized enzymes in diagnostics, Analytical Uses of Immobilized Biological Compounds for Detection, Medical and Industrial Uses 1988, pp. 71–82, https://doi.org/10.1007/978-94-009-2895-4_6.
[13] C.S. Pundir, V. Narwal, B. Batra, Determination of lactic acid with special emphasis on biosensing methods: a review, Biosens. Bioelectron. 86 (2016) 777–790, https://doi.org/10.1016/j.bios.2016.07.076.
[14] C.S. Pundir, V. Narwal, Biosensing methods for determination of triglycerides: a review, Biosens. Bioelectron. 100 (2018) 214–227, https://doi.org/10.1016/j.bios.2017.09.008.
[15] A. Mahadevan, S. Fernando, An improved glycerol biosensor with an Au-FeS-NAD-glycerol-dehydrogenase anode, Biosens. Bioelectron. 92 (2017) 417–424, https://doi.org/10.1016/j.bios.2016.10.085.
[16] T. Goriushkina, L. Shkotova, G. Gayda, H. Klepach, M. Gonchar, A. Soldatkin, et al., Amperometric biosensor based on glycerol oxidase for glycerol determination, Sensors Actuators B Chem. 144 (2010) 361–367, https://doi.org/10.1016/j.snb.2008.11.051.
[17] M. Niculescu, S. Sigina, E. Csöregi, Glycerol dehydrogenase based amperometric biosensor for monitoring of glycerol in alcoholic beverages, Anal. Lett. 36 (2003) 1721–1737, https://doi.org/10.1081/al-120023611.
[18] V. Narwal, C.S. Pundir, An improved amperometric triglyceride biosensor based on co-immobilization of nanoparticles of lipase, glycerol kinase and glycerol 3-phosphate oxidase onto pencil graphite electrode, Enzym. Microb. Technol. 100 (2017) 11–16, https://doi.org/10.1016/j.enzmictec.2017.01.009.
[19] C.S. Pundir, Enzyme Nanoparticles, Elsevier Press, London, 2015, https://doi.org/10.1016/c2014-0-03909-3.
[20] V. Narwal, P. Kumar, P. Joon, C.S. Pundir, Fabrication of an amperometric sarcosine biosensor based on sarcosine oxidase/chitosan/CuNPs/c-MWCNT/Au electrode for detection of prostate cancer, Enzym. Microb. Technol. 113 (2018) 44–51, https://doi.org/10.1016/j.enzmictec.2018.02.010.
[21] B. Batra, V. Narwal, C.S. Pundir, An amperometric lactate biosensor based on lactate dehydrogenase immobilized onto graphene oxide nanoparticles-modified pencil graphite electrode, Eng. Life Sci. 16 (2016) 786–794, https://doi.org/10.1002/elsc.201600082.
[22] E. Dede, Ö. Sağlam, Y. Dilgin, Sensitive voltammetric determination of niclosamide at a disposable pencil graphite electrode, Electrochim. Acta 127 (2014) 20–26, https://doi.org/10.1016/j.electacta.2014.01.153.
[23] G. Liu, Y. Lin, V. Ostatná, J. Wang, Enzyme nanoparticles-based electronic biosensor, Chem. Commun. (2005) 3481, https://doi.org/10.1039/b504943a.